

Phonon velocity and atomic interaction in superfluid ^4He

A. C. Olinto*

Fachbereich Physik, Universität Bremen, 2800 Bremen 33, West Germany

(Received 6 July 1987; revised manuscript received 14 December 1987)

From Ward identities that take into account the condensate reservoir, the velocity of long-wavelength phonons is obtained as a function of the condensate fraction and chemical potential. By introducing an effective He-atom scattering length $s(T)$ that increases with decreasing temperature, from $s(T=T_\lambda)=2.56 \text{ \AA}$ to $s(T=0)=3.13 \text{ \AA}$, excellent agreement between theory and experiment is obtained for the phonon velocity and chemical potential in the entire superfluid region. As a result, the condensate fraction is such that $n_0(T=0)=0.090$ and it exhibits a rapid buildup just below T_λ , in agreement with recent finite-temperature Green's-function Monte Carlo studies.

I. INTRODUCTION

The crucial role the Bose broken symmetry has in the field-theoretic description of superfluid ^4He is now well established. As first introduced by Bogoliubov¹ for weakly interacting systems and later generalized by Beliaev,² the order parameter is the ensemble average of the boson field $\langle\psi\rangle$. On the basis of this macroscopic wave function, Gavoret and Nozières³ were able to show that in the long-wavelength limit the density response and single-particle Green's functions display the same phonon spectrum. Griffin has recently discussed a more general approach to the role of $\langle\psi\rangle\neq 0$ in connection with the coupling of the density and field fluctuation spectra.⁴

The breaking of the gauge symmetry in terms of a real parameter ξ ($0<\xi\leq 1$) such that the zero-mode amplitudes satisfy the commutation relation $[b_0, b_0^\dagger]=1-\xi$, allows for microscopic fluctuations of the particles in the $k=0$ state.⁵ As a consequence, the continuity equation exhibits a source contribution and the additional terms that appear in the Ward identities may be interpreted as being due to the condensate reservoir.

The temperature dependence of the velocity of phonons in superfluid ^4He has long been of interest. Griffin has conjectured that the slight variation of the phonon velocity $c(T)$ with temperature is probably due to the changing condensate density.⁴ In Sec. II of this paper, the ξ formalism is used with the shielded-potential approximation^{6,7} (SPA) in the superfluid region, $T\leq T_\lambda$, to show that

$$c^2=(nU_0/m)[n_0-(1+\xi)\mu], \quad (1.1)$$

where U_0 is the interaction constant, m the He-atom mass, the total particle density n is taken as constant, $n_0(T)$ denotes the condensate fraction, and

$$\mu=\xi(n_0-2) \quad (1.2)$$

is the chemical potential measured in units of nU_0 .⁵ For $\xi=0$, only the first term on right-hand side of Eq. (1.1) survives and we recover the phonon velocity as determined by Szépfalussy and Kondor.⁷ The second term comes from the condensate reservoir ($\xi>0$), and because

of it the phonon velocity no longer vanishes at T_λ .

In the same framework of the ξ formalism and the SPA, the chemical potential per unit mass reads⁸

$$\bar{\mu}=(nU_0/m^*)\mu, \quad m^*\equiv\gamma m. \quad (1.3)$$

In Sec. III it is shown that the simultaneous fitting of both Eqs. (1.1) and (1.3) to the respective experimental data leads to a unique $n_0(T)$ for a given effective-mass parameter γ . This procedure also yields the temperature dependence of the interaction constant, which is the subject of Sec. IV.

II. LONG-WAVELENGTH PHONON VELOCITY

In the dielectric formulation of interacting Bose systems,^{7,9-11} the one-phonon excitation spectrum is determined by the poles of the full density-density response function through the zeros of the dielectric function,

$$1-U_0[\bar{\chi}_{nn}^C(k,w)+\bar{\chi}_{nn}^R(k,w)]=0, \quad (2.1)$$

where $\bar{\chi}_{nn}^C$ and $\bar{\chi}_{nn}^R$ are the improper and proper parts of the irreducible density-density correlation function, respectively; and since we are only interested in the long-wavelength limit, the interaction constant is taken as the Fourier transform of the interatomic potential. The improper contribution can be expressed in the form

$$\bar{\chi}_{nn}^C=\Lambda_\mu^n\bar{G}_{\mu\nu}\Lambda_\nu^n, \quad (2.2)$$

where $\bar{G}_{\mu\nu}$ are the irreducible Beliaev-type Green's functions and Λ_μ^n are the density vertex functions. The summation convention over repeated indices ($\mu, \nu=+, -$) is assumed and $\hbar=1$ is set throughout.

The proper part can be written in terms of regular functions from Ward identities that take into account the condensate reservoir. These identities are derived from the continuity equation with a source term due to the parameter ξ in the definition of the zero-mode amplitudes, such that

$$n_b\equiv\langle b_0^\dagger b_0\rangle V^{-1}=(1-\xi)\langle a_0^\dagger a_0\rangle V^{-1}+n_0, \quad (2.3)$$

where a_0 is the usual $k=0$ Bose annihilation operator, V denotes the volume of the system, and n_0 here is the con-

densate density (not fraction) that vanishes if $\xi=0$. From those Ward identities [Eqs. (2.22)–(2.25) in the second paper of Ref. 5, with $\xi n'_0 \equiv n_0$] it is straightforward to obtain

$$\begin{aligned} \omega^2 \bar{\chi}_{nn}^R = & \frac{k^2}{m} \left[\frac{m}{V k} \langle [J_k, \rho_k^\dagger] \rangle + m^{-1} \bar{\chi}_{JJ}^R \right. \\ & \left. - n_0^{1/2} k^{-1} \beta_\mu \Lambda_\mu^J - k^{-1} \bar{\chi}_{SJ}^R \right] \\ & - \omega \bar{\chi}_{Sn}^R - n_0^{1/2} \omega \beta_\mu \Lambda_\mu^n + \frac{\omega}{V} \langle [\rho_k, \rho_k^\dagger] \rangle, \end{aligned} \quad (2.4)$$

where ρ_k and J_k are the density and longitudinal-current operators, the subscripts and superscripts J and S in the correlation and vertex functions refer to the longitudinal-current and reservoir source, respectively, and $\beta_\mu \equiv \text{sgn} \mu$. In the thermodynamic limit, the last term of Eq. (2.4) vanishes and the first term within the parentheses equals the overall density n .

We now work out the general results (2.2) and (2.4) in the SPA. From previous results the vertex functions in this approximation are^{5,9–11}

$$\Lambda_\mu^n = n_0^{1/2}, \quad \Lambda_\mu^J = \frac{1}{2} k n_0^{1/2} \beta_\mu, \quad (2.5)$$

and since the irreducible self-energies vanish, $\bar{G}_{\mu\nu}$ equals the unperturbed Green's function,⁵

$$\bar{G}_{\mu\nu} = G_{\mu\nu}^0 = \delta_{\mu\nu} [(\text{sgn} \mu) \omega - \varepsilon_k + \mu]^{-1}, \quad (2.6)$$

where $\varepsilon_k = k^2/2m$ and μ here is the dimensional chemical potential (not in nU_0 units). From (2.5) and (2.6), Eq. (2.2) is readily evaluated,

$$\bar{\chi}_{nn}^C(k, \omega) = \frac{2n_0(\varepsilon_k - \mu)}{\omega^2 - (\varepsilon_k - \mu)^2}, \quad (2.7)$$

and Eq. (2.4) becomes

$$\begin{aligned} \bar{\chi}_{nn}^R = & m^{-1} \omega^{-2} k^2 (n + m^{-1} \bar{\chi}_{JJ}^R - n_0 - k^{-1} \bar{\chi}_{SJ}^R) \\ & - \omega^{-1} \bar{\chi}_{Sn}^R. \end{aligned} \quad (2.8)$$

We first consider the determination of $\bar{\chi}_{Sn}^R$. This is achieved through identical steps as in the evaluation of $\bar{\chi}_{SJ}^R$ [Eqs. (4.8)–(4.14) in Ref. 5]. Thus, we begin from its definition and factorize the imaginary time ($\tau \equiv i t$) ordered product, i.e.,

$$\begin{aligned} \chi_{Sn}(k, \tau) \equiv & - \langle T_\tau S_k(\tau) \rho_k^\dagger \rangle \\ = & 2\xi [\langle T_\tau a_k(\tau) a_k^\dagger \rangle \langle T_\tau b_0^\dagger(\tau) b_0 \rangle \\ & - \langle T_\tau a_{-k}^\dagger(\tau) a_{-k} \rangle \langle T_\tau b_0(\tau) b_0^\dagger \rangle] \\ & \times \sum_p \langle a_p^\dagger a_p \rangle, \end{aligned} \quad (2.9)$$

where ρ_k and S_k are defined by Eqs. (2.4) and (2.6) in Ref. 5. After substituting the unperturbed propagators by their well-known expressions,⁵ we Fourier analyze Eq. (2.9) and, subsequently, carry out the frequency summations by standard techniques. The frequency analytic

continuation then gives

$$\begin{aligned} \bar{\chi}_{Sn}^R(k, \omega) = & 2(1 - \xi) \xi n U_0 V^{-1} [N^0(\varepsilon_k) - N^0(0)] \\ & \times \left[\frac{1}{\omega - \varepsilon_k + \xi \mu} + \frac{1}{\omega + \varepsilon_k - \xi \mu} \right], \end{aligned} \quad (2.10)$$

where $N^0(\varepsilon_k)$ is the Bose distribution function. In the SPA one has $N^0(\varepsilon_k) = \langle a_k^\dagger a_k \rangle$ and $N^0(0) = \langle b_0^\dagger b_0 \rangle / (1 - \xi)$; hence, it follows from Eq. (2.3) that

$$[N^0(0) - N^0(\varepsilon_k)] / V = n_0 / (1 - \xi). \quad (2.11)$$

By substituting Eq. (2.11) in (2.10) we find

$$\bar{\chi}_{Sn}^R(k, \omega) = - \frac{4\xi n_0 n U_0 \omega}{\omega^2 - (\varepsilon_k - \xi \mu)^2}. \quad (2.12)$$

We consider next Eq. (2.8) in the low-frequency and long-wavelength limit, $(k, \omega) \rightarrow 0$. Talbot and Griffin¹¹ have shown that in the zero-frequency and long-wavelength limit the normal fluid density satisfies the sum rule

$$n_N = - \lim_{k \rightarrow 0} m^{-1} \bar{\chi}_{JJ}^R(k, 0). \quad (2.13)$$

This implies, in turn, a superfluid density⁵

$$n_S = n_0 + \lim_{k \rightarrow 0} k^{-1} \bar{\chi}_{SJ}^R(k, 0). \quad (2.14)$$

Hence, in the hydrodynamic limit the expression within the parentheses of Eq. (2.8) vanishes identically. On the other hand, in this limit Eqs. (1.2) and (2.12) imply that $\omega^{-1} \bar{\chi}_{Sn}^R = O(\xi^{-3})$, which is large since $\xi \ll 1$. As long as we end up with a phonon dispersion relation, and this will be the case, the factor in front of the parentheses in Eq. (2.8) is constant. Therefore, in the $(k, \omega) \rightarrow 0$ limit the dominant contribution to $\bar{\chi}_{nn}^R$ comes from the last term of Eq. (2.8):

$$\bar{\chi}_{nn}^R(k, \omega) = - \omega^{-1} \bar{\chi}_{Sn}^R, \quad (k, \omega) \rightarrow 0. \quad (2.15)$$

Combining now Eqs. (2.1), (2.7), (2.12), and (2.15), we finally obtain an equation for the zeros of the dielectric function:

$$\frac{2n_0 U_0 (\varepsilon_k - \mu)}{\omega^2 - (\varepsilon_k - \mu)^2} + \frac{4\xi n_0 n U_0^2}{\omega^2 - (\varepsilon_k - \xi \mu)^2} = 1. \quad (2.16)$$

For convenience we make dimensionless the quantities that enter Eq. (2.16) by measuring energies and momenta in units of nU_0 and $(mnU_0)^{1/2}$, respectively. After some algebra Eq. (2.16) can be rewritten as

$$\omega^4 - A(k) \omega^2 + B(k) = 0, \quad (2.17)$$

where the coefficients have the form

$$A(k) = \sum_{i=0}^2 \alpha_i \varepsilon_k^{2-i} \quad \text{and} \quad B(k) = \sum_{i=0}^4 \beta_i \varepsilon_k^{4-i}, \quad (2.18)$$

with the α_i 's and β_i 's given by

$$\begin{aligned}
\alpha_0 &= 2, \quad \alpha_1 = 2[n_0 - (1 + \xi)\mu], \\
\alpha_2 &= 4\xi n_0 - 2n_0\mu + (1 + \xi^2)\mu^2, \quad \beta_0 = 1, \\
\beta_1 &= \alpha_1, \\
\beta_2 &= 2n_0[2\xi - (1 + 2\xi)\mu] + (1 + 4\xi + \xi^2)\mu^2, \\
\beta_3 &= 2\xi\mu\{n_0[(2 + \xi)\mu - 4] - (1 + \xi)\mu^2\}, \\
\beta_4 &= \xi\mu^2[2n_0(2 - \xi\mu) + \xi\mu^2].
\end{aligned}
\tag{2.19}$$

Here again n_0 and μ denote, respectively, the condensate fraction and the dimensionless chemical potential (1.2). With regard to the magnitude of the coefficients in (2.19), we recall that $n_0 \lesssim \xi$, which implies $\mu = O(\xi)$ and, consequently, α_i and β_i are of $O(\xi^i)$.

On the basis of the $k \rightarrow 0$ and $\xi \ll 1$ limit, a phonon dispersion relation results if one neglects terms of $O(\epsilon_k^3)$ or $O(\xi^2)$. In this case we eliminate in Eq. (2.17) the contributions from $B(k)$ and α_2 , the latter being the energy gap which is inherent to the ξ formalism in the SPA.⁵ Thus Eq. (2.17) reduces to a (dimensionless) Bogoliubov-type energy spectrum, namely,

$$w^2 = \alpha_0 \epsilon_k^2 + \alpha_1 \epsilon_k \quad (k \rightarrow 0, \xi \ll 1), \tag{2.20}$$

which gives immediately the (dimensional) phonon velocity

$$c^2 = \frac{1}{2}(nU_0/m)\alpha_1. \tag{2.21}$$

Taking into account the expression for α_1 in Eq. (2.19), this result becomes identical to Eq. (1.1).

To illustrate the above results we let $n_0(T=0) = 0.090$. This choice, which will be justified in Sec. IV, implies $\xi = 0.1036$ [Eq. (2.6) in Ref. 8], and the values of $n_0(T)$ are then obtained [Eq. (4.19) in the second paper of Ref. 5] from known values of $n_s(T)$.¹² Therefore, the second factor in Eq. (1.1) can be readily evaluated, whereas the factor $(nU_0/m)^{1/2}$ is chosen so that¹³ $c(T=0) = 238.21$ m sec⁻¹. In Table I the calculated $c(T)$ is compared with the experimental data.¹²⁻¹⁴ The agreement is excellent

TABLE I. Phonon velocity at various temperatures and saturated vapor pressure. Experimental values from Refs. 12 ($0 < T < T_\lambda$), 13 ($T=0$) and 14 ($T=T_\lambda$), calculated from Eq. (1.1) for $n_0(T=0) = 0.090$.

T (K)	c (m sec ⁻¹)	
	Calc.	Expt.
0	238.21	238.21
1.20	237.37	237.4
1.30	236.80	236.8
1.40	235.98	236.1
1.50	234.83	235.2
1.60	233.27	234.0
1.70	231.22	232.7
1.80	228.54	231.0
1.90	225.06	228.8
2.00	220.53	225.8
2.10	214.20	221.8
T_λ	205.11	217.1

up to about $T = 1.5$ K. Although the theoretic values depart from the measurements as T increases, they represent a substantial improvement with regard to the previous result due to Szépfalussy and Kondor that predicts a vanishing $c(T \rightarrow T_\lambda)$.⁷

An increase (decrease) in the initial choice of $n_0(T=0)$ provides higher (smaller) values of $c(T)$ in the interval $(0, T_\lambda]$. Thus, an inspection of Table I shows that $n_0(T=0) = 0.090$ gives a better fit than any $n_0(T=0) < 0.090$. This is to be contrasted with the case $n_0(T=0) = 0.062$ that results from the best fit of $\bar{\mu}(T)$.⁸ On the other hand, $n_0(T=0) \sim 0.18$ fits $c(T_\lambda)$ [and, by construction, $c(T=0)$], but at temperatures $0 < T < T_\lambda$ the calculated values exceed the experimental error.

In the remaining sections we adopt the following approach: by assuming *ab initio* that Eqs. (1.1) and (1.3) do correctly describe $c(T)$ and $\bar{\mu}(T)$, what would then be the resultant condensate fraction and interatomic potential.

III. THE CONDENSATE FRACTION

In this section we show that the fitting of Eqs. (1.1) and (1.3) to the experimental measurements is a convenient way to extract the condensate fraction. Dividing one equation by the other we obtain a dimensionless relation,

$$\gamma \alpha_1(T) / 2\mu(T) = c^2(T) / \bar{\mu}(T). \tag{3.1}$$

The function μ and α_1 depend on ξ both explicit and implicitly through n_0 , so that the substitution of the right-hand side of Eq. (3.1) by the measured values defines a constraint surface $f(T, \xi, \gamma) = 0$. To this end we use the following data: the phonon velocity as given by the second column in Table I and the chemical potential¹⁵ $m\bar{\mu}(T=0) = -7.160$ K, that is, $\bar{\mu}(T=0) = -14.878$ J g⁻¹ ($= -86.828$ K² Å²), and, at temperatures in the interval 1.2 K $\leq T \leq 2.1$ K, the values as tabulated by Maynard in 0.1 K steps.¹² All these quantities refer to the saturated vapor pressure. Figure 1 exhibits the relationship

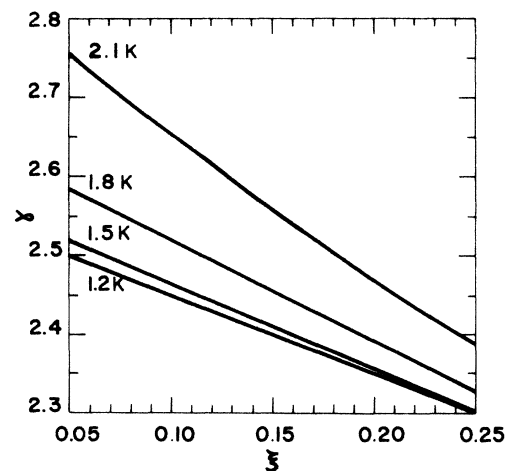


FIG. 1. Relationship between symmetry-breaking and effective-mass parameters at given temperatures, calculated by Eq. (3.1), where $c(T)$ and $\bar{\mu}(T)$ correspond to the measured values found in Ref. 12.

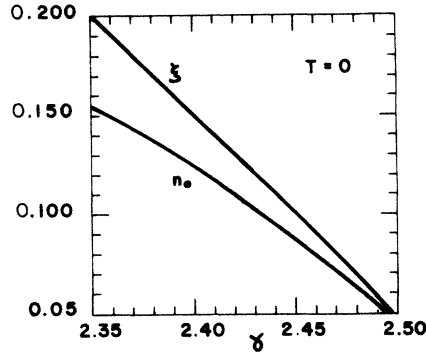


FIG. 2. Symmetry-breaking and effective-mass parameters calculated similarly as in Fig. 1 for $T=0$, with $c(0)$ and $\bar{\mu}(0)$ from Refs. 13 and 15. Condensate fraction corresponding to ξ ($T=0$), calculated from Eq. (4.19) in Ref. 5.

between ξ and γ at given temperatures. The $T=0$ K curve is hardly distinguishable from the $T=1.2$ K one and is plotted in Fig. 2 together with the associated n_0 ($T=0$). Clearly, a fixed γ defines the T dependence of ξ and conversely. Since it is natural to assume a constant effective mass, a knowledge of n_0 at any T specifies γ , and the latter implies $\xi(T)$ in the entire superfluid region. We illustrate this with three examples: $n_0(T=0)=0.06$, 0.09, and 0.12, which yield (Fig. 2) $\gamma=2.483$, 2.447, and 2.406, respectively. The corresponding $\xi(T)$ and $n_0(T)$ for each case are shown in Figs. 3 and 4.

If one makes the plausible assumption that $n_0(T) \geq n_0(T')$, $T < T'$, then the case $n_0(T=0)=0.06$ is ruled out by a simple inspection of Fig. 4. By this criterion a lower bound of 8.3% is found for the condensate fraction at absolute zero.

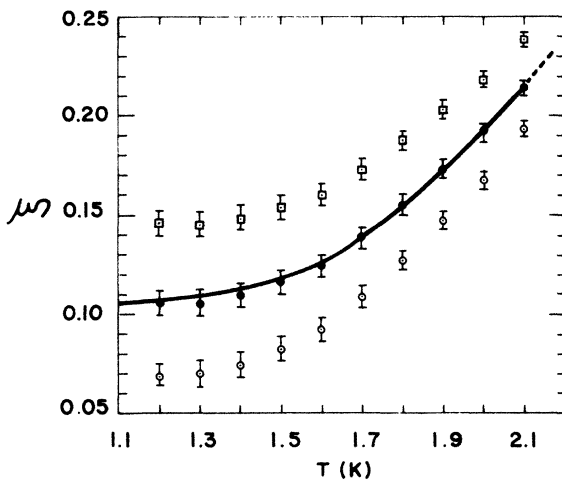


FIG. 3. Symmetry-breaking parameter vs temperature. \circ : $n_0(T=0)=0.06$, $\gamma=2.483$; \bullet : $n_0(T=0)=0.09$, $\gamma=2.447$; \square : $n_0(T=0)=0.12$, $\gamma=2.406$. The errors indicated are related to the uncertainties in the measured values of $c(T)$ and $\bar{\mu}(T)$ in Ref. 12. Solid curve: $\xi(T)$ that gives $n_0(T)$ represented by the solid curve of Fig. 4. Dashed curve: extrapolation of the solid curve to T_λ .

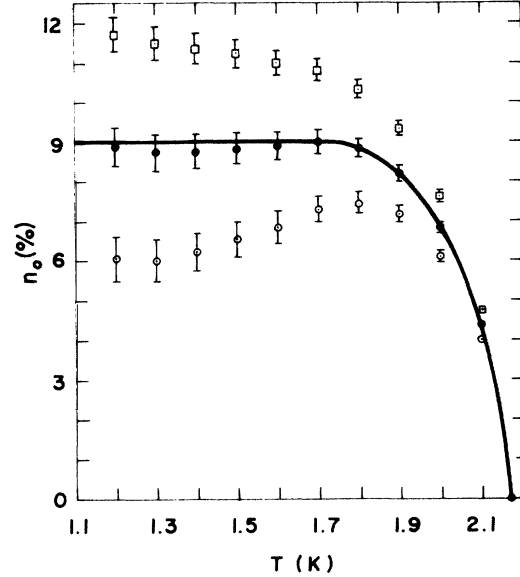


FIG. 4. Condensate fraction vs temperature calculated from Eq. (4.19) of Ref. 5 and corresponding to each set of $\xi(T)$ given in Fig. 3.

IV. THE INTERATOMIC POTENTIAL

By construction, Eq. (3.1) is independent of the interaction constant and furnishes a family of $n_0(T)$'s whose members are specified by γ . In order to actually fit $c(T)$ and $\bar{\mu}(T)$, one must, in addition, find out the quantities

$$v \equiv (nU_0/m)^{1/2}, \quad (4.1)$$

$$g \equiv nU_0/m^* = v^2/\gamma. \quad (4.2)$$

For definiteness we take for $n_0(T)$, and the associated $\xi(T)$, the solid curves represented in Figs. 4 and 3, respectively, which correspond to $\gamma=2.447$ and $n_0(T=0)=0.090$, as in Sec. II.

This choice is suggested by Green's-function Monte Carlo calculations¹⁶ and, as will be seen below, turns out to be a judicious one. The function $v(T)$ represented in Fig. 5 was obtained by matching Eqs. (1.3) and (4.2) with the measured^{12,15} $\bar{\mu}(T)$ as shown in Fig. 6. By using this $v(T)$ we compare in Fig. 7 the calculated $c(T)$, Eqs. (1.1) and (4.1), with the experimental values.¹²⁻¹⁴ Since to our knowledge data on $\bar{\mu}(T_\lambda)$ is not available, which prevents a determination of $\xi(T_\lambda)$ from Eq. (3.1), we have circumvented this problem by calculating $v(T_\lambda)$ from Eq. (1.1) with¹⁴ $c(T_\lambda)=217.1$ m sec⁻¹ and the extrapolated result $\xi(T_\lambda)=0.231$ as indicated by the dashed curve in Fig. 3.

By using the above determined values of $v(T)$ and the He-atom mass in (4.1), one sees that nU_0 increases from 39.9 K ($T=T_\lambda$) to 88.55 K ($T=0$). These are difficult to be interpreted physically since the He-atom parameters yield $nU_0 \sim 8.6$ K. By the same token, we recall that Aldrich and Pines¹⁷ found $nU_0 \sim 27.3$ K. We next show that $v(T)$ can nevertheless be rewritten in terms of an effective interaction that is suited to a physical interpretation.

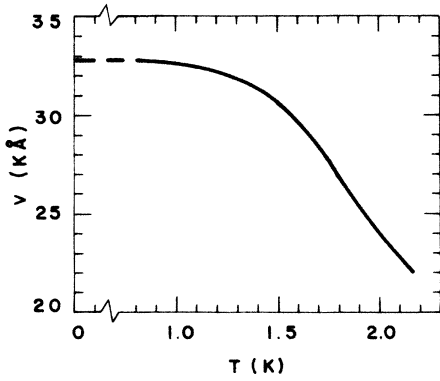


FIG. 5. Temperature dependence of v , Eq. (4.1), which fits calculated and measured values of $\bar{\mu}(T)$ as shown in Fig. 6.

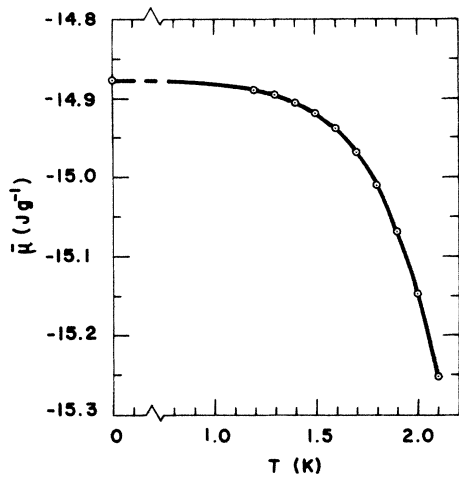


FIG. 6. Chemical potential per unit mass vs temperature. Solid curve: Eqs. (1.3) and (4.2) with $v(T)$ as given in Fig. 5. \circ : experimental values from Refs. 15 ($T=0$) and 12 ($T>0$).

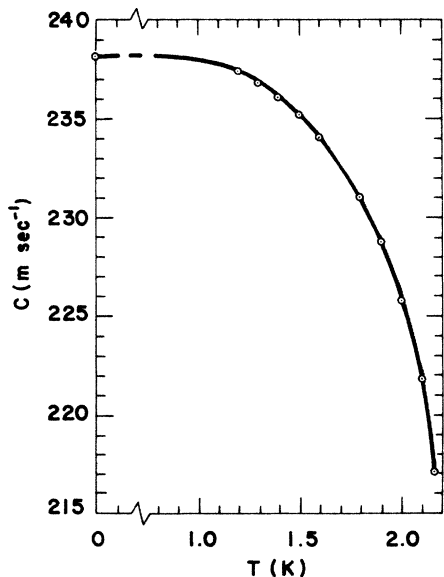


FIG. 7. Phonon velocity vs temperature. Solid curve: Eqs. (1.1) and (4.1) with $v(T)$ as given in Fig. 5. \circ : experimental values from Refs. 13 ($T=0$), 12 ($0 < T < T_\lambda$), and 14 ($T=T_\lambda$).

Accordingly, we first notice that the right-hand side of (4.1) comes from the product of nU_0 with $(mnU_0)^{1/2}$, which are the respective natural units of energy and length used in Sec. II. This leads us to introduce new energy and length parameters, nU'_0 and s , defined by

$$v \equiv nU'_0 s, \quad U'_0 \equiv 4\pi s / m. \quad (4.3)$$

Consequently, one has

$$v(T) = (4\pi n / m) s^2(T); \quad (4.4)$$

and $s(T)$ is shown in Fig. 8 with the constant factor in (4.4) taken at $T=T_\lambda$:

$$4\pi n / m = 3.353 \text{ \AA}, \quad [n(T_\lambda) = 0.022 \text{ \AA}^{-3}]. \quad (4.5)$$

In particular, $s_\lambda \equiv s(T=T_\lambda) = 2.56 \text{ \AA}$ equals the He-atom hard-core diameter and $s_0 \equiv s(T=0) = 3.1264 \text{ \AA}$ is close to, but smaller than the average interatomic distance.¹⁸ Similarly, one finds $nU'_0(T=T_\lambda) = 8.59 \text{ K}$ and $nU'_0(T=0) = 10.483 \text{ K}$. These physical values allow one to interpret $s(T)$ as an effective scattering length for the He atoms in the superfluid region, whereas in the normal phase $s(T > T_\lambda) = s_\lambda$, as indicated in Fig. 8. Equation (4.4) can then be rewritten as

$$v(T) = n\sigma(T)/m, \quad \sigma(T) \equiv 4\pi s^2(T), \quad (4.6)$$

where $\sigma(T)$ is the total effective cross section. Likewise, from Eqs. (4.1) and (4.6) the interaction constant becomes

$$U_0 = n\sigma^2 / m. \quad (4.7)$$

Finally, we remark that the calculated $c(T)$ and $\bar{\mu}(T)$ still fall within the experimental errors for any $n_0(T=0)$ chosen within the interval $\sim 0.06-0.12$. The corresponding s_λ and s_0 parameters are shown in Fig. 9. It is relevant that $n_0(T=0) = 0.09$ is located halfway between the interval limits, which is a clear indication of the best fit.

V. CONCLUDING REMARKS

In summary it was shown that an analysis of the phonon velocity and chemical potential leads to well-defined $n_0(T)$ and $s(T)$ for a given γ . This latter parameter is chosen so that $s(T_\lambda)$ equals the real He-atom cross-

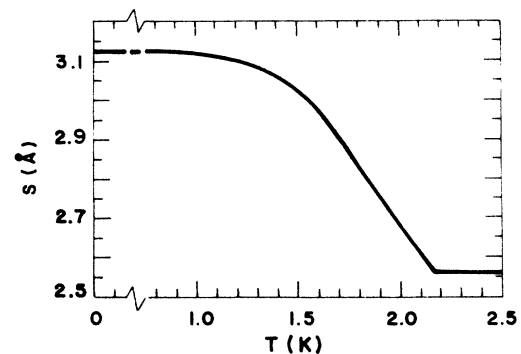


FIG. 8. Effective scattering length vs temperature, Eqs. (4.4) and (4.5), with $v(T)$ as given in Fig. 5.

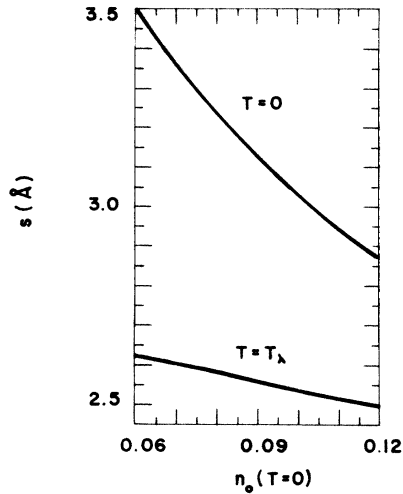


FIG. 9. Effective scattering lengths $s_0(T=0)$ and $s_\lambda(T=T_\lambda)$ as functions of $n_0(T=0)$.

section diameter. The fact that this scheme implies $n_0(T=0)=0.09$ strengthens the Green's-function Monte Carlo results¹⁶ which is, incidentally, close to the original value obtained by Penrose and Onsager from a plausible ground-state wave function.¹⁹

In previous studies of the condensate,^{5,8} the symmetry-breaking parameter ξ was regarded as a constant throughout the superfluid region, and as a consequence $n_0(T)$ did not display such a rapid buildup just below T_λ as seen in Fig. 4. Moreover, a constant ξ gives $n_0(T)$ values⁸ that are close to the ones furnished by an empirical formulation due to Svensson, Sears, and Griffin.²⁰ However, by reanalyzing the procedure of extracting the condensate fraction from inelastic neutron scattering, Griffin²¹ obtains values of $n_0(T)$ that are considerably larger at high T and smaller at low T . Furthermore, Griffin⁴ has also pointed out the rapid increase of $n_0(T)$ in a recent finite-temperature computer simulation carried out by Ceperley and Pollock.²²

With regard to a plausible physical explanation for the increase of the effective scattering length, we recall that London had estimated the zero-point energy for the two limiting cases of very small and very high densities.²³ In both cases it was found that this energy increases with the hard-core diameter. In fact, we have found in Sec. IV that the effective interaction constant is such that

$$n[U'_0(T=0) - U'_0(T=T_\lambda)] = 1.89 \text{ K}, \quad (5.1)$$

while the zero-point energy associated with the two-particle interaction at $T=0$ is estimated to be

$$2n^{2/3}m^{-1} = 1.90 \text{ K}. \quad (5.2)$$

In this view, the underlying reason for the T dependence of the effective scattering length is accounted for by the increase in the dominant role of the zero-point energy from $T=T_\lambda$ down to $T=0$.

To see how this energy might affect the interatomic potential, we extend an argument due to Landau and used by Bogoliubov in his original work.¹ In that gas model of superfluidity the interaction is primarily due to binary collisions, and in the evaluation of the Fourier amplitudes of the two-particle potential the free-particle waves are to be replaced by the exact wave functions obtained in the solution of the Schrödinger equation. Thus, in principle, the zero-point motion manifests itself in the Fourier coefficient of the potential via the exact wave functions.

We finally remark that an increase of the scattering length below the λ point lends itself to a qualitative description of the steep fall of viscosity in this region. As emphasized by London,²³ liquid He I at low temperatures and under low pressures has a viscosity of the type usually found in gases and not in liquids. Hence, the coefficient of viscosity is expected to vary linearly with the mean-free path, and the latter with the reciprocal of the scattering cross section. As the temperature enters the superfluid region the cross-section increase contributes additionally to the lowering of the viscosity. At absolute zero, although 91% of the particles carry momentum, there is no transport mechanism that leads to a finite viscosity. If one assumes a statistical preference for a radial distribution function of a T_d^2 lattice type, then the average interparticle distance is of the order of $2^{-1/6}n^{-1/3} \sim 3.18 \text{ \AA}$.^{23,24} On the other hand, we have found that $s(T=0) \sim 3.13 \text{ \AA}$, which means that the mean-free path is vanishingly small, and so is the viscosity's transport mechanism. Despite the simple arguments involved, this physical picture serves the purpose of showing that an increase of the scattering length is compatible with the phenomenon of superfluidity.

ACKNOWLEDGMENTS

I would like to thank Professor C. C. Noack for his hospitality at the Department of Physics at the University of Bremen and the Deutscher Akademischer Austauschdienst for financial support.

*Present and permanent address: Laboratório Nacional de Computação Científica, C.P. 56018, 22290 Rio de Janeiro, Rio de Janeiro, Brazil.

¹N. Bogoliubov, *J. Phys. (Moscow)* **11**, 23 (1947).

²S. T. Beliaev, *Zh. Eksp. Teor. Fiz.* **34**, 417 (1958) [*Sov. Phys.—JETP* **7**, 289 (1958)]; **34**, 433 (1958) [**7**, 299 (1958)].

³J. Gavoret and P. Nozières, *Ann. Phys. (N.Y.)* **28**, 349 (1964).

⁴A. Griffin, *Can. J. Phys.* (to be published).

⁵A. C. Olinto, *Phys. Rev. B* **33**, 1849 (1986); **34**, 6159 (1986).

⁶A. Griffin and T. H. Cheung, *Phys. Rev. A* **7**, 2086 (1973).

⁷P. Szépfalusy and I. Kondor, *Ann. Phys. (N.Y.)* **82**, 1 (1974).

⁸A. C. Olinto, *Phys. Rev. B* **35**, 4771 (1987).

⁹S. K. Ma and C. W. Woo, *Phys. Rev.* **159**, 165 (1967).

¹⁰V. K. Wong and H. Gould, *Ann. Phys. (N.Y.)* **83**, 252 (1974).

¹¹E. Talbot and A. Griffin, *Ann. Phys. (N.Y.)* **151**, 71 (1983); *Phys. Rev. B* **29**, 3952 (1984).

- ¹²J. Maynard, *Phys. Rev. B* **14**, 3868 (1976).
- ¹³J. Brooks and R. J. Donnelly, *J. Phys. Chem. Ref. Data* **6**, 51 (1977).
- ¹⁴G. Ahlers, *Phys. Rev. A* **8**, 530 (1973).
- ¹⁵E. M. Lifshitz and L. P. Pitaevskii, *Statistical Physics* (Pergamon, New York, 1980), Part 2, p. 87.
- ¹⁶M. H. Kalos, M. A. Lee, P. A. Whitlock, and G. V. Chester, *Phys. Rev. B* **24**, 115 (1981).
- ¹⁷C. H. Aldrich and D. Pines, *J. Low Temp. Phys.* **25**, 677 (1976).
- ¹⁸The precision at T_λ is reduced due to the extrapolation procedure regarding $\xi(T_\lambda)$.
- ¹⁹O. Penrose and L. Onsager, *Phys. Rev.* **104**, 576 (1956).
- ²⁰E. C. Svensson, V. F. Sears, and A. Griffin, *Phys. Rev. B* **23**, 4493 (1981); E. C. Svensson and V. F. Sears, *Physica (Utrecht)* **137B**, 126 (1986).
- ²¹A. Griffin, *Phys. Rev. B* **32**, 3289 (1985); *Physica (Utrecht)* **136B**, 177 (1986).
- ²²D. M. Ceperley and E. L. Pollock, *Phys. Rev. Lett.* **56**, 351 (1986).
- ²³F. London, *Superfluids* (Dover, New York, 1965), Vol. II.
- ²⁴W. H. Keesom and K. W. Taconis, *Physica (Utrecht)* **5**, 270 (1938).